

RSC Advances



This is an *Accepted Manuscript*, which has been through the Royal Society of Chemistry peer review process and has been accepted for publication.

Accepted Manuscripts are published online shortly after acceptance, before technical editing, formatting and proof reading. Using this free service, authors can make their results available to the community, in citable form, before we publish the edited article. This *Accepted Manuscript* will be replaced by the edited, formatted and paginated article as soon as this is available.

You can find more information about *Accepted Manuscripts* in the [Information for Authors](#).

Please note that technical editing may introduce minor changes to the text and/or graphics, which may alter content. The journal's standard [Terms & Conditions](#) and the [Ethical guidelines](#) still apply. In no event shall the Royal Society of Chemistry be held responsible for any errors or omissions in this *Accepted Manuscript* or any consequences arising from the use of any information it contains.

Cite this: DOI: 10.1039/c0xx00000x

www.rsc.org/xxxxxx

ARTICLE TYPE

Novel pure Pnma-P2₁2₁2₁ ferroelastic phase transition of 1,4-diisopropyl-1,4-diazonia-bicyclo[2.2.2]octane tetra-chlorobromo-M(II) (M=Mn and Co)

Li-Zhuang Chen,^{*,a} Deng-Deng Huang^a Qi-Jian Pan^a and Jia-Zhen Ge^b

Received (in XXX, XXX) Xth XXXXXXXXX 20XX, Accepted Xth XXXXXXXXX 20XX
DOI: 10.1039/b000000x

Two novel phase transition compounds Dip-DABCO tetra-chlorobromo-M(II) (M = Mn and Co), (Dip-DABCO = 1,4-diisopropyl-1,4-diazonia-bicyclo[2.2.2]octane) C₁₂H₂₆N₂·MnBrCl₃ (**1**) and (C₁₂H₂₆N₂)₄·(CoBr_{1.25}Cl_{2.75})₄ (**2**) were synthesized and their structures have been determined by means of single-crystal X-ray diffraction. The two compounds are isomorphous. Differential scanning calorimetry (DSC) measurements detected that compound **1** and **2** underwent a reversible phase transition at ca. 245.2 K with a hysteresis of 4.4 K width and ca. 222.3 K with a hysteresis of 5.5 K width respectively. The variable-temperature single crystal X-ray diffraction data suggested that the phase transition undergoes from a high crystallographic symmetry with space group of Pnma to the low symmetry state with space group of P2₁2₁2₁, that is, Landau symmetry breaking occurs with a pure GPT (mmm-222). The ordering of twisting motions of 1,4-diazoniabicyclo[2,2,2]octane ring may drive the phase transition.

Introduction

There is currently a great deal of interest in searching for new temperature-triggered solid-to-solid phase transition materials (SSPTMs) due to their potential applications in data communication, signal processing, signal processing, phase shifters and environment-monitoring, etc.¹ Preparing new temperature-triggered molecular-based phase transition materials is crucial not only for the theoretical study of structure–property relationship but also for the exploration of novel physical properties.^{2–3} One of the biggest challenges in searching for phase transition materials is always the rational design of novel systems.⁴ By constructing special types of organic–inorganic hybrid complexes may be an effective method of the design of ideal phase transition materials. Hybrid organic–inorganic coordination complexes possess the advantageous properties of both organic and inorganic compounds. Their topologies can be rationally designed by taking advantage of well-defined metal coordination geometries in combination with carefully chosen distorted or disordered anions which are benefit for the adjustment and design of ideal phase transition materials.⁵ Recently, hybrid inorganic–organic phase transition materials have been widely studied.⁶ Among which, phase transition materials containing 1,4-diazabicyclo-[2.2.2]octane (dabco) have demonstrated specific responses to external electric or temperature stimuli, they have provided a lot of room for us to explore phase transition materials based on the ligand. More recently, a series of metal-organic compounds assembled by 1,4-

diazabicyclo-[2.2.2]octane which undergo the structure transitions have been synthesized by Xiong et al.⁷ All these findings reveal that the dabco component would afford the potential to design and construct new functional electric ordering materials because of its striking features as donor-acceptor of proton or order-disorder structural transformation. However, 1,4-diisopropyl-1,4-diazonia-bicyclo[2.2.2]octane dibromide, as a potential bridging ligand, has rarely been studied regarding the coordination chemistry. Taking all these into consideration, as a continuation of our systematic studies of phase transitions,⁸ we report herein two new compounds 1,4-diisopropyl-1,4-diazonia-bicyclo[2.2.2]octane tetra-chlorobromo-manganese(II) (**1**) and 1,4-diisopropyl-1,4-diazonia-bicyclo[2.2.2]octane tetra-chlorobromo-cobalt (II) (**2**) with reversible structural phase transition properties based on the novel ligand, which were characterized by variable-temperature single crystal X-ray diffraction, differential scanning calorimetry (DSC) and TGA measurements.

Experimental

Materials and measurements

All reagent-grade chemicals and solvents were obtained from commercial sources and used without further purification. Infrared spectra of compound **1** and **2** were recorded on a SHIMADZU IR prestige-21 FTIR-8400S spectrometer in the range of 4000–500 cm⁻¹ with samples in the form of potassium bromide pellets (Fig. S1 and S2, Supporting Information). X-ray powder diffraction data were collected by a Siemens D5005

diffractometer with Cu-K α radiation ($\lambda=1.5418 \text{ \AA}$). Powder X-ray diffraction (PXRD) patterns of **1** and **2** (Fig. S3 and S4, Supporting Information) at room temperature matched very well those simulated from the single-crystal structures, confirming the phase purity of **1** and **2** respectively. Elemental analyses were

taken on a Perkin-Elmer 240C elemental analyzer. Thermo gravimetric analyses (TGA) of **1** and **2** were conducted on a NETZSCH TG 209 F3 thermo gravimeter with a heating rate of 10 K/min in N₂ atmosphere (Fig. S5 and S6, Supporting Information).

Table 1 Crystallographic data for **1** and **2** at RTP and LTP

	1 (296K)	1 (150K)	2 (296K)	2 (150K)
Empirical formula	C ₁₂ H ₂₆ BrCl ₃ MnN ₂	C ₁₂ H ₂₆ BrCl ₃ MnN ₂	C ₄₈ H ₁₀₄ Br ₅ Cl ₁₁ Co ₄ N ₈	C ₄₈ H ₁₀₄ Br ₅ Cl ₁₁ Co ₄ N ₈
Formula weight	439.55	439.55	1818.61	1818.61
Crystal system	Orthorhombic	Orthorhombic	Orthorhombic	Orthorhombic
Space group	Pnma	P2 ₁ 2 ₁	Pnma	P2 ₁ 2 ₁
<i>a</i> (Å)	13.778(3)	13.6378(11)	13.7347(15)	13.5796(9)
<i>b</i> (Å)	10.235(2)	10.1863(8)	10.1454(11)	10.0792(7)
<i>c</i> (Å)	13.238(3)	13.1566(11)	13.1412(14)	13.0655(9)
α (°)	90	90	90	90
β (°)	90	90	90	90
γ (°)	90	90	90	90
<i>V</i> (Å ³)	1866.7(7)	1827.7(3)	1831.1(3)	1788.3(2)
<i>Z</i>	4	4	1	1
<i>D_c</i> (g/m ³)	1.564	1.597	1.649	1.689
μ (mm ⁻¹)	3.267	3.337	4.056	4.153
<i>F</i> (000)	892	892	918	918
θ range [°]	2.13 to 25.68	2.15 to 25.67	2.14 to 25.67	2.16 to 25.67
Collected reflections	13530	13842	13326	13624
Unique reflections	1879	3461	1840	3389
<i>R</i> ₁ , <i>wR</i> ₂ [<i>I</i> > 2 σ (<i>I</i>)]	0.0510, 0.1677	0.0314, 0.1068	0.0687, 0.2379	0.0402, 0.1076
<i>R</i> ₁ , <i>wR</i> ₂ [all data]	0.0642, 0.1835	0.0330, 0.1118	0.0815, 0.2653	0.0417, 0.1119
GOF	1.490	0.985	1.166	1.074
Largest peak and hole (e ⁻ Å ⁻³)	1.213, -1.073	0.649, -0.786	1.573, -2.674	1.276, -1.406

0.71073 Å). A pale yellow rod-like crystal of **1** with approximate

Synthesis of **1**

Manganese chloride tetrahydrate (1.97 g, 10 mmol) and 1,4-diisopropyl-1,4-diazonia-bicyclo[2.2.2]octane dibromide (3.6 g, 10 mmol) were mixed in aqueous solution (30 ml) (Scheme 1). After being stirred for 20 min in air, the reaction mixture solution was evaporated slowly at room temperature for 3 days, and pale yellow rod-like crystals were obtained in 58% yield (based on Manganese chloride). IR spectra of compound **1**: 3393(s), 3017(s), 2978(m), 1633(m), 1478(s), 1407(s), 1328(m), 1171(m), 1117(s), 1061(m), 989(w), 893(m), 851(s), 830(s), 815(m), 665(w), 589(w), 555(w). Anal. (%) calcd for C₁₂H₂₆BrCl₃MnN₂: C, 32.79; H, 5.96; N, 6.37; Found: C, 32.61; H, 5.85; N, 6.28.

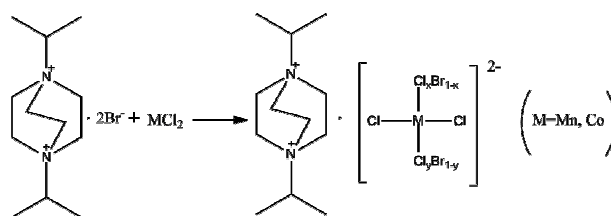
Synthesis of **2**

Cobalt (II) chloride hexahydrate (2.38 g, 10 mmol) and 1,4-diisopropyl-1,4-diazonia-bicyclo[2.2.2]octane dibromide (3.6 g, 10 mmol) were mixed in aqueous solution (30 ml) (Scheme 1). After being stirred for 20 min in air, the reaction mixture solution was evaporated slowly at room temperature for 5 days, and blue rod-like crystals were obtained in 55% yield (based on Cobalt (II) chloride). IR spectra of compound **2**: 3439(s), 3016(s), 2975(m), 1638(m), 1478(s), 1402(s), 1326(m), 1174(m), 1110(s), 1063(m), 1032(w), 970(w), 894(m), 861(s), 827(s), 798(w), 683(w), 585(w), 550(w). Anal. (%) calcd for C₄₈H₁₀₄Br₅Cl₁₁Co₄N₈: C, 31.70; H, 5.76; N, 6.16; Found: C, 31.61; H, 5.64; N, 6.08.

Single-crystal X-ray diffraction measurements

Single-crystal X-ray data of compounds **1** and **2** were performed on a Bruker SMART-APEX II CCD with Mo-K α radiation ($\lambda =$

0.71073 Å). A pale yellow rod-like crystal of **1** with approximate dimensions 0.40 × 0.40 × 0.20 mm was used in data collection at 296 and 150 K respectively. And a blue rod-like crystal of **2** with approximate dimensions 0.30 × 0.30 × 0.20 mm was used in data collection at 296 and 150 K similarly. Data processing including empirical absorption correction was performed using SADABS. The structures of **1** and **2** was solved by direct methods and refined by the full-matrix method based on *F*² by means of the SHELXLTL software package.⁹ Non-H atoms were refined anisotropically using all reflections with *I* > 2 σ (*I*). All H atoms were found in the difference maps. However, carbon-bond H atoms were added geometrically and refined using riding model with *U*_{iso} = 1.2U_{eq}. Asymmetric units and packing views were drawn with DIAMOND (Brandenburg and Putz, 2005). Distances and angles between some atoms were calculated using DIAMOND and other calculations were carried out using SHELXLTL. Crystallographic data and structure refinements of **1** and **2** at the 296 K and 150 K phases are listed in Table 1 respectively.



Scheme 1 Synthesis of compound **1** and **2**.

DSC Measurement

DSC runs of crystal **1** (17.5 mg) and **2** (24.26 mg) were recorded using a NETZSCH DSC 200 F3 instrument from 280 to 180 K and 270 to 190 K respectively with a heating rate of 15 K/min and 10 K/min respectively on cooling/heating under nitrogen at atmospheric pressure in aluminum crucibles.

Results and discussion

DSC

Differential Scanning Calorimetry (DSC) measurement is one of the thermodynamic methods that detect the dependence of reversible phase transition on temperature. Heating the crystalline sample of **1** shows a main endothermic peak at 249.6 K and a main exothermic peak on cooling at 245.2 K (Fig. 1), with the enthalpy changes of $\Delta H_h = 0.6832$ J/g and $\Delta H_c = 0.5646$ J/g respectively. The step-like anomaly of these two main peaks and the thermal hysteresis of 4.4 K reveal a reversible phase transition of **1**. Similarly, heating the crystalline sample of **2** shows a main endothermic peak at 227.8 K and a main exothermic peak on cooling at 222.3 K (Fig. 2), with the enthalpy changes of $\Delta H_h = 0.4253$ J/g and $\Delta H_c = 0.3964$ J/g respectively. The step-like anomaly of these two main peaks and the thermal hysteresis of 5.5 K reveal a reversible phase transition of **2**.

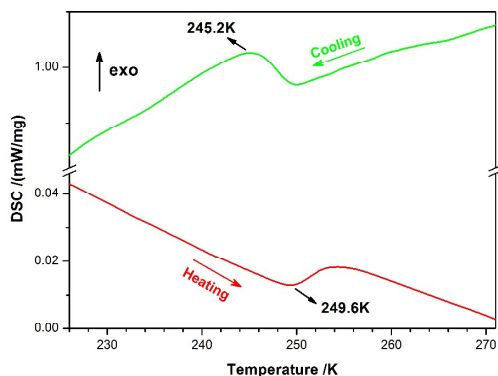


Fig.1 DSC curves of **1** obtained in a heating-cooling mode

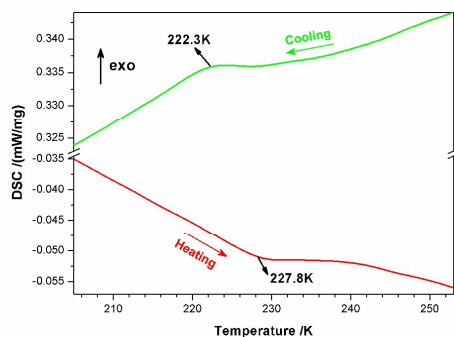


Fig.2 DSC curves of **2** obtained in a heating-cooling mode

Crystal structure of **1**

The phase transition of **1** was further confirmed by determining variable-temperature crystal structures at room-temperature phase and low-temperature phase, respectively (Fig. 3a-b). The crystal structure of **1** at room temperature (296 K) is orthorhombic with a centrosymmetric space group of Pnma and the point group D_{2h} .

When the temperature decreases to 150 K, **1** transforms to another orthorhombic crystal structure with the chiral space group $P2_12_12_1$ and the point group D_2 . Thereafter the crystal structures of **1** were compared at 296 K and 150 K. At room temperature (296 K), the crystals are in the orthorhombic space group Pnma (No. 62). When cooled to 150 K, the crystals become orthorhombic space group $P2_12_12_1$ (No. 19). The crystals show no obvious changes at the two temperatures. Molecular volume decreases from $1866.7(7) \text{ \AA}^3$ in the RTP to $1827.7(3) \text{ \AA}^3$ in the LTP.

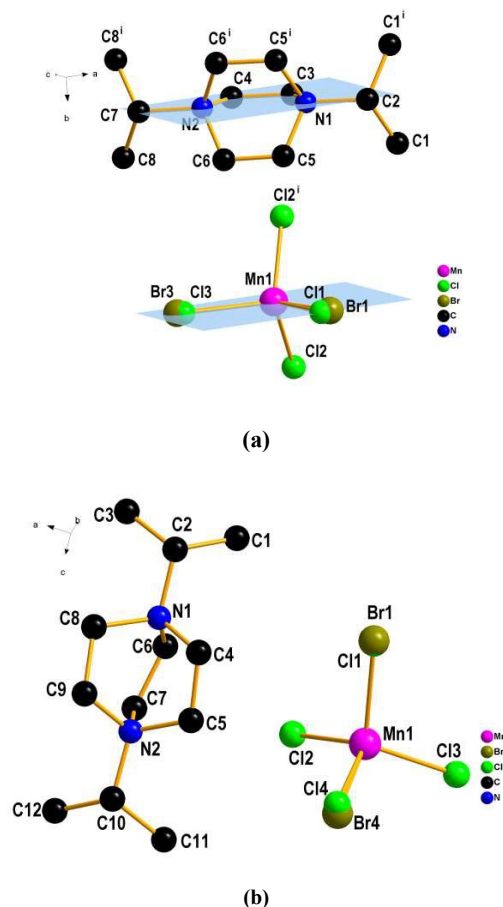
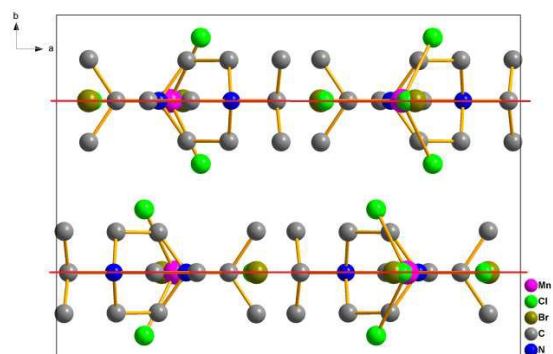


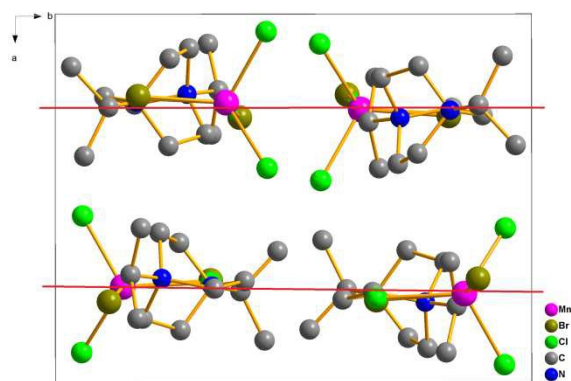
Fig.3 View of the asymmetric unit of **1** with atomic numbering scheme at (a) 296 K and (b) 150 K.

In the room-temperature phase (RTP, 296 K), the structure of 1,4-diisopropyl-1,4-diazonia-bicyclo[2.2.2]octane tetrachlorobromo-manganese(II) consists of the 1,4-diisopropyl-1,4-diazonia-bicyclo[2.2.2]octane dications and tetrahedral MnBrCl_3 anions (Fig. 3a). The Mn(II) ion adopts a distorted tetrahedral geometry, which coordinates to the two equivalent Cl atoms, and two disorder of halogen (Br/Cl) atoms which exhibit substitutional disorder of halogen atoms in the asymmetric unit, the halogen atom bonded to Mn has 0.5 occupancy for Cl and 0.5 for Br. In the asymmetric unit of the RTP structure, the 9 non-hydrogen atoms ((Br3\Cl3), (Br1\Cl1), Mn1, C7, N2, C4, C3, N1 and C2) located in a mirror plane with occupancy factor of 0.5, other non-H atoms apart from the above mirror plane can be produced by a $(x, -y+3/2, z)$ symmetry transformation. It is notable

that the bond lengths of the Mn–Br and Mn–Cl bonds are strikingly different (Table S1), that is, the substitutional disorder Br is 2.452(3) Å (Mn1–Br1) and the other 2.462(12) Å (Mn1–Br3). The distance of Mn1–Cl2 is 2.3706(10) Å, the bond length is obviously shorter than that of the substitutional disorder Cl1, 2.459(18) Å (Mn1–Cl1), and it is a little longer than that of the substitutional disorder Cl3, 2.332(12) Å (Mn1–Cl3).



(a)



(b)

Fig. 4 Unit cell packing diagrams of **1** at (a) 296 K and (b) 150 K.

In the lower-temperature phase (LTP, 150 K) crystal structure, the Mn(II) ions still adopts the distorted tetrahedral geometry (Fig. 3b). However, the bond lengths of the three Mn–Cl bonds are all different: Mn1–Cl1 = 2.390(5) Å, Mn1–Cl2 = 2.3909(8) Å, Mn1–Cl3 = 2.3536(10) Å and Mn1–Cl4 = 2.448(13) Å (Table S2). The bond lengths of the two Mn–Br bonds are 2.436(4) Å (Mn1–Br1) and 2.476(2) Å (Mn1–Br4), respectively. Meanwhile, conformations of the rings of the dabco ligand show a little difference at the both temperature phases. The values of the N–C–C–N torsion angles are 0° in the RTP and 23.3(4)°, 22.7(4)°, 24.9(4)° in the LTP, respectively. In the LTP unit cell (Fig. 4b), the 9 non-hydrogen atoms ((Br3\Cl3), (Br1\Cl1), Mn1, C7, N2, C4, C3, N1 and C2) apparently deviate from the crystallographic mirror plane.

X-ray crystal structures of **1** were measured at 290 K, 280K, 270 K, 260, 250 K, 240K, 230 K, 220, 210 K, 200, 190 K, 180 K and 170 K. The cell parameters of **1** measured at LTP are slightly

30 different from those measured at RTP, as is shown in Fig. 5.

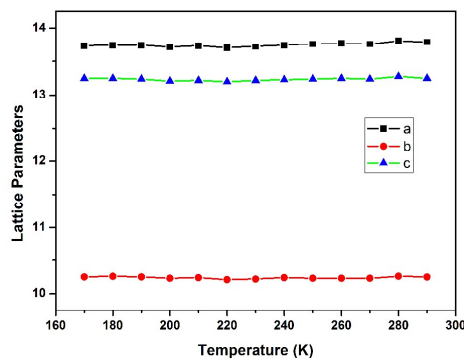


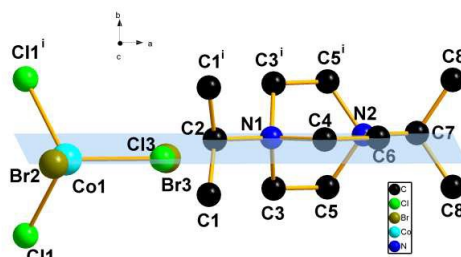
Fig. 5 Temperature dependence of unit-cell lengths parameters of **1**

TGA of **1**

35 To study the thermal stability of **1** and to further confirm its molecular formula, thermogravimetric (TG) analysis was performed in N₂ on sample of complex **1** in the range of 25–1000 °C (Fig. S5). The TGA curve indicate that compound **1** exhibits relatively high thermal stability. The decomposition 40 temperature is around 263.8 °C, corresponding to the release of organic ligands. Upon temperature increase, the structure of **1** begins to collapse.

Crystal structure of **2**

The phase transition of **2** was further confirmed by determining 45 variable-temperature crystal structures at room-temperature phase and low-temperature phase, respectively (Fig. 6a-b). The crystal structure of **2** at room temperature (296 K) is orthorhombic with a centrosymmetric space group of Pnma and the point group D_{2h}. When the temperature decreases to 150 K, **2** transforms to 50 another orthorhombic crystal structure with the chiral space group P2₁2₁2₁ and the point group D₂. Thereafter the crystal structures of **2** were compared at 296 K and 150 K. At room temperature (296 K), the crystals are in the orthorhombic space group Pnma (No. 62). When cooled to 150 K, the crystals become 55 orthorhombic space group P2₁2₁2₁ (No. 19). The crystals show no obvious changes at the two temperatures. Molecular volume decreases from 1831.1(3) Å³ in the RTP to 1788.3(2) Å³ in the LTP.



(a)

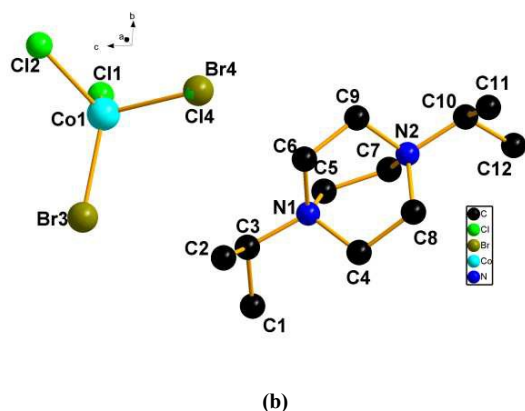
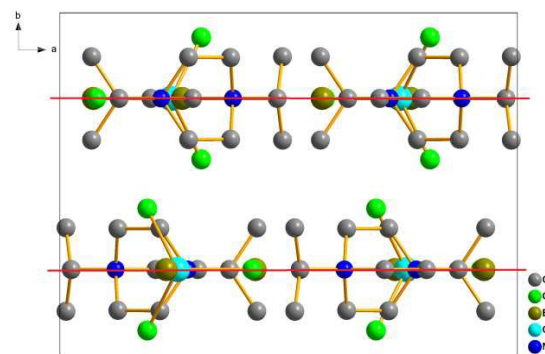


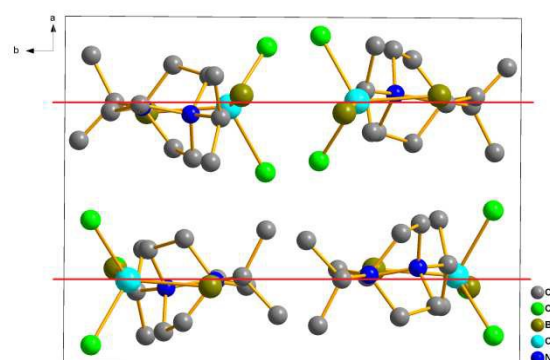
Fig. 6 View of the asymmetric unit of **2** with atomic numbering scheme at (a) 296 K and (b) 150 K.

In the room-temperature phase (RTP, 296 K), the structure of 1,4-diisopropyl-1,4-diazonia-bicyclo[2.2.2]octane tetra-chlorobromocobalt(II) consists of the 1,4-diisopropyl-1,4-diazonia-bicyclo[2.2.2]octane dications and tetrahedral $\text{CoBr}_{1.25}\text{Cl}_{2.75}$ anions (Fig. 6a). The Co(II) ion adopts a distorted tetrahedral geometry, which coordinates to the two equivalent Cl atoms, one Br atom and one disorder of halogen (Br/Cl) atoms which exhibit substitutional disorder of halogen atoms in the asymmetric unit, the halogen atom bonded to Co has 0.75 occupancy for Cl and 0.25 for Br. In the asymmetric unit of the RTP structure, the 9 non-hydrogen atoms (Br2, (Br3/Cl3), Co1, C7, N2, C6, C4, N1 and C2) located in a mirror plane with occupancy factor of 0.5, other non-H atoms apart from the above mirror plane can be produced by a $(x, -y+1/2, z)$ symmetry transformation. It is notable that the bond lengths of the Co–Br and Co–Cl bonds are strikingly different (Table S3), that is, the substitutional disorder Br is 2.39(3) Å (Co1–Br3) and the other 2.3733(15) Å (Co1–Br2), which are comparable to those bond lengths of the Mn–Br in **1**. The distance of Co1–C11 is 2.2855(13) Å, the bond length is a bit longer than that of the substitutional disorder Cl3, 2.26(2) Å (Co1–Cl3).

In the lower-temperature phase (LTP, 150 K) crystal structure, the Co(II) ions still adopts the distorted tetrahedral geometry (Fig. 6b). However, the bond lengths of the three Co–Cl bonds are all different: Co1–C11 = 2.2734(14) Å, Co1–C12 = 2.3048(12) Å and Co1–C14 = 2.323(12) Å (Table S4). The bond lengths of the two Co–Br bonds are 2.3926(8) Å (Co1–Br3) and 2.341(14) Å (Co1–Br4), respectively, which also provide a direct comparison to compound **1**. Meanwhile, conformations of the rings of the dabco ligand show a little difference at the both temperature phases. The values of the N–C–C–N torsion angles are 0° in the RTP and 22.7(6)°, 22.2(6)°, 24.6(6)° in the LTP, respectively. In the LTP unit cell (Fig. 7b), the 9 non-hydrogen atoms (Br2, (Br3/Cl3), Co1, C7, N2, C6, C4, N1 and C2) apparently deviate from the crystallographic mirror plane.



(a)



(b)

Fig. 7 Unit cell packing diagrams of **2** at (a) 296 K and (b) 150 K.

X-ray crystal structures of **2** were measured at 290 K, 270 K, 250 K, 230 K, 220, 210 K, 200, 190 K and 170 K. The cell parameters of **2** measured at LTP are slightly different from those measured at RTP which are similar with **1** (Fig. S6).

TGA of **2**

To study the thermal stability of **2** and to further confirm its molecular formula, thermogravimetric (TG) analysis was performed in N_2 on sample of complex **2** in the range of 25–1000 °C (Fig. S7). The TGA curve indicate that compound **2** exhibits relatively high thermal stability as compound **1**. The decomposition temperature is around 230 °C, corresponding to the release of organic ligands. Upon temperature increase, the structure of **2** begins to collapse.

Compound **1** and **2** undergo a phase transition (ca. $T=245.2$ K and ca. $T=222.3$ K respectively) from a room-temperature phase with a space group of Pnma to a low-temperature one with a chiral space group $P2_12_12_1$ respectively. During the transition from RTP to LTP, Landau symmetry breaking occurs with a pure GPT (mmm-222).¹⁰ In other words, the eight symmetric elements (E, C₂, 2C₂', i, σ_h , 2 σ_v) at RTP are halved into four symmetry elements (E, C₂, 2C₂') at LTP owing to the loss of i, σ_h and 2 σ_v . The mirror symmetry in [010] is broken and inversion center disappear. The 2-fold screw axis remains unchanged, leading to the final low-temperature space group $P2_12_12_1$. It is noted that the

number of the symmetry operations in Pnma decreases by half from 8 [(1) 1; (2) 2(0, 0, 1/2) 1/4, 0, z; (3) 2(0, 1/2, 0) 0, y, 0; (4) 2(1/2, 0, 0) x, 1/4, 1/4; (5) $\bar{1}$ 0, 0, 0; (6) a x, y, 1/4; (7) m x, 1/4, z; (8) n(0, 1/2, 1/2) 1/4, y, z.] to 4 [(1) 1; (2) 2(0, 0, 1/2) 1/4, 0, z; (3) 2(0, 1/2, 0) 0, y, 1/4; (4) 2(1/2, 0, 0) x, 1/4, 0] in P₂1₂1₂1, in

perfect agreement with the symmetry breaking analysis(Fig. 8). A variation-temperature-crystal engineering strategy is successfully combined with Landau phase transition theory in the application of ferroelastics design.

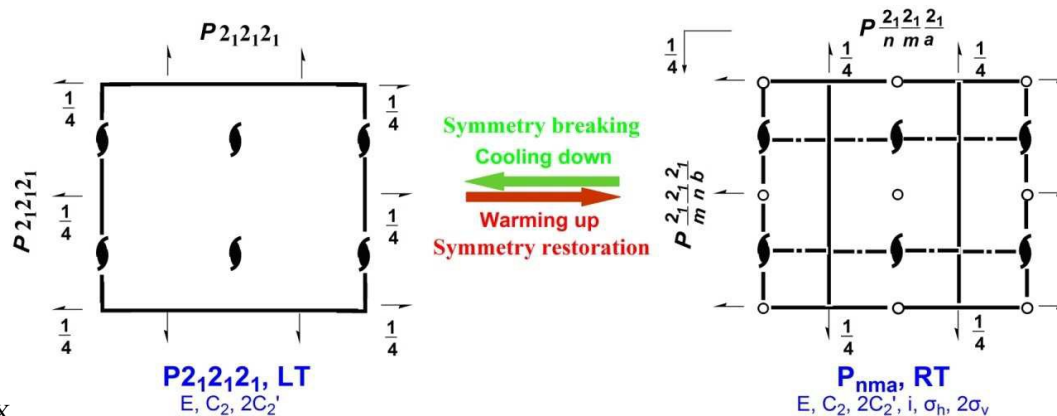


Fig. 8 Changes of symmetry operations of **1** and **2** from Pnma at RTP to P₂1₂1₂1 at LTP.

Conclusions

In summary, DSC, variable-temperature structural analysis and TGA revealed that compound **1** and **2** underwent a reversible phase transition while being discontinuous at ca. 245.2 K and ca. 222.3 K respectively. Crystal structures of **1** and **2** obtained at room-temperature phase and low-temperature phase revealed that they reversibly transformed from the RTP space group of Pnma to the LTP space group of P₂1₂1₂1. During the transition from RTP to LTP, Landau symmetry breaking occurs with a pure GPT (mmm-222) in both compound **1** and **2**. Owing to the ordering of twisting motions of 1,4-diisopropyl-1,4-diazonia-bicyclo[2.2.2]octane ion, conformations of the rings of dabco differed evidently between RTP and LTP phases. The ordering of twisting motions of dabco ring probably drove the phase transition.

Acknowledgements

This work was funded by the National Natural Science Foundation of China (Grant No. 21201087), JiangSu Province NSF BK20131244, the Foundation of Jiangsu Educational Committee (11KJB150004) and sponsored by Qing Lan Project of Jiangsu province and Jiangsu Overseas Research & Training Program for University Prominent Young & Middle-aged Teacher and Presidents, the Innovation Program of Graduate Students in Jiangsu Province (SJZZ_0142).

Notes and references

^a School of Environmental and Chemical Engineering, Jiangsu University of Science and Technology, Zhenjiang 212003, China.

E-mail: clz1977@sina.com

^b Ordered Matter Science Research Center, Southeast University, Nanjing, 210096, P.R. China.

Electronic supplementary information (ESI) available: Crystallographic information (in CIF format) of compounds **1** and **2** at room-temperature phase and low-temperature phase respectively, these data have been deposited at the Cambridge Crystallography Data Centre : CCDC 1026402 for 296 K, 1026403 for 150 K of **1**; CCDC 972355 for 296 K,

972354 for 150 K of **2**. In addition, IR, PXRD and TGA of compound **1** and **2** in electronic supplementary information respectively.

Reference

- (a) D. Lencer, M. Salinga and M. Wuttig, *Adv. Mater.*, 2011, **23**, 2030–2058; (b) M. Salinga and M. Wuttig, *Science*, 2011, **332**, 543; (c) H. Zheng, J. B. Rivest, T. A. Miller, B. Sadtler, A. Lindenberg, M. F. Toney, L.-W. Wang, C. Kisielowski and A. P. Alivisatos, *Science*, 2011, **333**, 206–209; (d) J. F. Scott and C. A. P. Dearaujo, *Science*, 1989, **246**, 1400–1405.
- (a) J. F. Scott, *Science*, 2007, **315**, 954–959; (b) S. Horiuchi and Y. Tokura, *Nature Material*, 2008, **7**, 357–366; (c) I. R. Evans, J. A. K. Howard and J. S. O. Evans, *Cryst. Growth Des.*, 2008, **8**, 1635–1639; (d) G.-C. Xu, X.-M. Ma, L. Zhang, Z.-M. Wang, S. Gao, *J. Am. Chem. Soc.*, 2010, **132**, 9588–9590.
- (a) M. Szafranski and M. Jarek, *CrystEngComm*, 2013, **15**, 4617–4623; (b) Z.-H. Sun, J.-H. Luo, T.-L. Chen, L.-N. Li, R.-G. Xiong, M.-L. Tong and M.-C. Hong, *Adv. Funct. Mater.*, 2012, **22**, 4855–4861; (c) Q. Ye, T. Akutagawa, H.-Y. Ye, T. Hang, J.-Z. Ge, R.-G. Xiong, S.-i. Noro and T. Nakamura, *CrystEngComm*, 2011, **13**, 6185–6191.
- (a) Z.-H. Sun, X.-Q. Wang, J.-H. Luo, S.-Q. Zhang, D.-Q. Yuan and M.-C. Hong, *J. Mater. Chem. C*, 2013, **1**, 2561–2567; (b) Y. Zhang, H.-Y. Ye, D.-W. Fu and R.-G. Xiong, *Angew. Chem.*, 2014, **126**, 2146–2150.
- H. Zhang, X.-M. Wang, K.-C. Zhang and B. K. Teo, *Coord. Chem. Rev.*, 1999, **183**, 157–195.
- (a) H.-Y. Ye, H.-L. Cai, J.-Z. Ge and R.-G. Xiong, *Inorg. Chem. Commun.*, 2012, **17**, 159–162; (b) Y. Zhang, W. Zhang, S.-H. Li, Q. Ye, H.-L. Cai, F. Deng, R.-G. Xiong and S. P. D. Huang, *J. Am. Chem. Soc.*, 2012, **134**, 11044–11049.
- (a) Y. Zhang, W.-Q. Liao, H.-Y. Ye, D.-W. Fu and R.-G. Xiong, *Cryst. Growth Des.*, 2013, **13**, 4025–4030; (b) W. Zhang, H.-Y. Ye, H.-L. Cai, J.-Z. Ge, R.-G. Xiong, S.-D. Huang, *J. Am. Chem. Soc.*, 2010, **132**, 7300–7302. (c) H.-Y. Ye, J.-Z. Ge, F. Chen and R.-G. Xiong, *CrystEngComm*, 2010, **12**, 1705–1708.
- (a) L.-Z. Chen, D.-D. Huang, J.-Z. Ge and F.-M. Wang, *CrystEngComm*, 2014, **16**, 2944–2949; (b) L.-Z. Chen, H. Zhao, J.-Z. Ge, R.-G. Xiong and H.-W. Hu, *Cryst. Growth Des.*, 2009, **9**, 3828–3831; (c) H.-Y. Ye, L.-Z. Chen and R.-G. Xiong, *Acta Crystallogr. B*, 2010, **66**, 387–395.

- 9 (a) G. M. Sheldrick, SHELXL-97, Program for Crystal Structure Solution, University of Gottingen, Germany, 1997; (b) G. M. Sheldrick, SHELXS-97, Program for Crystal Structure Refinement, University of Gottingen, Germany, 1997.
- 5 10 (a) M. J. Tellot, A. López-Echarri, J. Zubillagat, I. Ruiz-Lamea, F. J. Zúñigat, G. Madariaga and A. Gómez-Cuevast, *J. phys.:Condens. Matter*, 1994, **6**, 6751–6760; (b) A. Gómez-Cuevast, J. M. Pérez Mato, M. J. Tello, G. Madariaga, J. Fernández, López Echarri, *Phys. Rev. B*, 1984, **29**, 2655–2663; (c) S. Prosandeev, I. A. Kornev, L. Bellaïche, *Phys. Rev. Lett.*, 2011, **107**, 117602; (d) S. Hirotsu, *J. Phys. C: Solid State Phys.*, 1975, **8**, L12–L16.
- 10